

First-principles study of moderate phonon-mediated pairing in high-pressure monoclinic phase of BiS_2-based superconductors

Jie Cheng(程杰), Yu-Lan Cheng(程玉兰), Bin Li(李斌), and Sheng-Li Liu(刘胜利)
Citation: Chin. Phys. B, 2023, 32 (**10**): 107401. DOI: 10.1088/1674-1056/accd56
Journal homepage: http://cpb.iphy.ac.cn; http://iopscience.iop.org/cpb

What follows is a list of articles you may be interested in

A ten-fold coordinated high-pressure structure in hafnium dihydrogen with increasing superconducting transition temperature induced by enhancive pressure

Yan-Qi Wang(王妍琪), Chuan-Zhao Zhang(张传钊), Jin-Quan Zhang(张金权), Song Li(李松), Meng Ju(巨濛), Wei-Guo Sun(孙伟国), Xi-Long Dou(豆喜龙), and Yuan-Yuan Jin(金园园)
Chin. Phys. B, 2023, 32 (**9**): 097402. DOI: 10.1088/1674-1056/acc934

Focused-ion-beam assisted technique for achieving high pressure by uniaxial-pressure devices

Di Liu(刘迪), Xingyu Wang(王兴玉), Zezhong Li(李泽众), Xiaoyan Ma(马肖燕), and Shiliang Li(李世亮)
Chin. Phys. B, 2023, 32 (**4**): 047401. DOI: 10.1088/1674-1056/acac1a

Photothermal-chemical synthesis of P-S-H ternary hydride at high pressures

Tingting Ye(叶婷婷), Hong Zeng(曾鸿), Peng Cheng(程鹏), Deyuan Yao(姚德元), Xiaomei Pan(潘孝美), Xiao Zhang(张晓), and Junfeng Ding(丁俊峰)
Chin. Phys. B, 2022, 31 (**6**): 067402. DOI: 10.1088/1674-1056/ac5604

Pressure-induced anomalous insulating behavior in frustrated iridate $La_3Ir_3O_{11}$

Chun-Hua Chen(陈春华), Yong-Hui Zhou(周永惠), Ying Zhou(周颖), Yi-Fang Yuan(袁亦方), Chao An(安超), Xu-Liang Chen(陈绪亮), Zhao-Ming Tian(田召明), and Zhao-Rong Yang(杨昭荣)
Chin. Phys. B, 2021, 30 (**6**): 067402. DOI: 10.1088/1674-1056/abf100

Superconducting anisotropy and vortex pinning in $CaKFe_4As_4$ and $KCa_2Fe_4As_4F_2$

A B Yu(于奥博), Z Huang(黄喆), C Zhang(张驰), Y F Wu(吴宇峰), T Wang(王腾), T Xie(谢涛), C Liu(刘畅), H Li(李浩), W Peng(彭炜), H Q Luo(罗会仟), G Mu(牟刚), H Xiao(肖宏), L X You(尤立星), and T Hu(胡涛)
Chin. Phys. B, 2021, 30 (**2**): 027401. DOI: 10.1088/1674-1056/abcf98

First-principles study of moderate phonon-mediated pairing in high-pressure monoclinic phase of BiS_2-based superconductors

Jie Cheng(程杰)[1,†], Yu-Lan Cheng(程玉兰)[2], Bin Li(李斌)[1,‡], and Sheng-Li Liu(刘胜利)[1]

[1] *School of Science, New Energy Technology Engineering Laboratory of Jiangsu Province, Nanjing University of Posts and Telecommunications, Nanjing* 210023, *China*

[2] *College of Electronic and Optical Engineering & College of Flexible Electronics (Future Technology), Nanjing University of Posts and Telecommunications, Nanjing*, 210023, *China*

(Received 12 February 2023; revised manuscript received 7 April 2023; accepted manuscript online 17 April 2023)

Isotope effect on superconductive transition temperature (T_c) is an essential indicator to examine whether the mechanism of superconductors is conventional. Unconventional isotope effect of BiS_2-based superconductors has been previously reported in ambient-pressure tetragonal phase. However, to comprehensively ascertain the nature of superconductivity, the investigation of BiS_2-based system in high-pressure structure is highly desirable. In this work, we carried out the first-principles calculations of phonon spectra and superconductivity in high-pressure monoclinic phase of $LaO_{0.5}F_{0.5}BiS_2$ with ^{32}S and ^{34}S, and observed that the corresponding isotope coefficient is $0.13 \leq \alpha \leq 0.20$. This value is much greater than that of BiS_2-based superconductors in ambient-pressure phase, but slightly smaller than that of conventional MgB_2. Taking into account the calculated T_c lower than experimental results, we finally conclude that the moderate phonon-mediated pairing plays a significant role in forming superconductivity of BiS_2-based system in high-pressure phase, moreover, the cooperative multiple paring interactions should also be considered.

Keywords: BiS_2-based superconductor, high pressure, isotope effect, phonon-mediated pairing

PACS: 74.62.Fj, 74.25.Kc, 31.15.A–, 74.70.–b **DOI:** 10.1088/1674-1056/accd56

1. Introduction

Superconductivity in layered crystal structure such as cuprates,[1] iron-pnictides,[2] and MgB_2,[3] has aroused enormous research interest. A new family of layered BiS_2-based system has triggered off another wave of extensive studies since its discovery in 2012. As the first member, the compound of $Bi_4O_4S_3$ was reported,[4] then the *Re*OBiS_2- (*Re*: rare earth),[5–9] SrFBiS_2-,[10] *Re*O*M*S_2 (M = Sb and In)-,[11,12] and $La_2O_2M_4S_6$ (M = Pb, Bi, Ag)-type superconductors[13–15] have been discovered successively. Here, the basic structural unit of BiS_2-based compounds is the BiS_2 layer, which is analogous to the Cu–O planes in cuprates and the Fe–*A* (A = P, As, Se, Te) planes in iron-pnictides.[1,16] Of these BiS_2-based compounds, the *Re*OBiS_2-type is mostly studied owing to their simple structure and easy carrier doping control. For example, in $LaO_{1-x}F_xBiS_2$, the partial substitutions of F^- for O^{2-} sites generate electron carriers, and the maximum transition temperature (T_c) is observed to be 2.5 K when $x = 0.5$ at ambient pressure.[17] Interestingly, by applying external pressure, T_c abruptly increases to a maximal value of 10.7 K, which is caused by the structural phase transition from tetragonal phase ($P4/nmm$, ambient-pressure) to monoclinic phase ($P2_1/m$, high-pressure).[18] Moreover, band structure calculations indicate the presence of strong Fermi surface nesting at the wave vector (π, π), which is the hallmark of iron-pnictides.[19,20] Therefore, the superconducting mechanism in BiS_2-based system may be expected to resemble that of iron-pnictides, although the mechanism of superconductivity in iron-pnictides is still in dispute.

According to the Bardeen–Cooper–Schrieffer (BCS) theory,[21] the T_c of a phonon-mediated conventional superconductor is proportional to its phonon frequency, and it is very sensitive to the isotope mass (M) of the constituent elements. This is the so-called isotope effect. Furthermore, the relationship between T_c and isotope mass satisfies $T_c \sim M^{-\alpha}$,[22] in which α is the isotope exponent, and $\alpha \sim 0.5$ is expected according to BCS theory. Therefore, the isotope effect can be considered as an essential indicator to investigate whether the mechanism of superconductors is conventional. For instance, α has been reported to be ~ 0.5 for the conventional superconductors, such as (Ba,K)BiO_3 ($\alpha_O \sim 0.5$),[23] doped fullerene ($\alpha_C \sim 0.5$),[24] and MgB_2 ($\alpha_B \sim 0.3$).[25] In high-T_c superconductors with unconventional mechanisms, α generally deviates from 0.5 (e.g. near-zero α_O in cuprates,[26] and even negative α_{Fe} in iron-pnictides[27]).

For this new BiS_2-based system, the fundamental question is whether the superconductivity can be understood within a conventional electron–phonon coupling framework. Hence, several investigations concerning the isotope effect of BiS_2-based compounds have been proposed. By replacing S element in $Bi_4O_4S_3$ with ^{32}S and ^{34}S, the isotope exponent α_S is estimated to be in a range: $-0.1 < \alpha_S < 0.1$.[28]

[†]Corresponding author. E-mail: chengj@njupt.edu.cn
[‡]Corresponding author. E-mail: libin@njupt.edu.cn

© 2023 Chinese Physical Society and IOP Publishing Ltd

A similar unconventional isotope effect is also observed in $LaO_{0.6}F_{0.4}BiSSe$ with BiSSe-type superconducting layers, in which the change of T_c between the ^{76}Se sample and ^{80}Se sample is apparently smaller than that expected from the photon-mediated mechanism.[29] Very recently, Yamashita *et al.* pointed out that under high pressure, the superconducting mechanism can be transformed from unconventional to conventional one by breaking the structural symmetry in superconducting BiS_2 layers.[30] It should be noted that these above-mentioned results of unconventional superconducting mechanism are based on the low-T_c tetragonal structures at ambient-pressure. Therefore, it is highly desirable to investigate the isotope effect on the high-pressure monoclinic phase, which may present an important clue to the understanding of the pairing mechanism in BiS_2-based superconductors.

In this work, we perform first-principles phonon calculations for the high-pressure monoclinic structure of $LaO_{0.5}F_{0.5}BiS_2$. The changes in T_c between ^{32}S sample and ^{34}S sample are observed, furthermore, the corresponding isotope exponent of $0.13 \leq \alpha \leq 0.20$ is obtained. These findings prompt the high-pressure structure of $LaO_{0.5}F_{0.5}BiS_2$ to be a moderate phonon-mediated superconductor, which is quite different from the unconventional isotope effect of ambient-pressure phase.

2. Computational method

The lattice data of $LaO_{0.5}F_{0.5}BiS_2$ were constructed by Materials Studio software. Starting from the initial lattice parameters, we performed the full structural optimization including both the lattice parameters and atomic positions. Phonon calculations were carried out by using density functional perturbation theory (DFPT) method via QUANTUM ESPRESSO program and a standard solid-state pseudopotential (SSSP).[31–33] The exchange–correlation energy was described by the Perdew–Burke–Ernzerhof (PBE) functional based on generalized gradient approximation (GGA).[34] For self-consistent calculation, $8\times8\times8$ k-point grid was used with an energy cutoff of 30 Ry (1 Ry = 13.6056923 eV) for the wave function and 300 Ry for the charge density. Dynamical matrices and electron–phonon coupling were calculated on a 4 $\times4\times4$ q-point mesh. Then, a dense $24\times$ 24 $\times24$ grid was used for evaluating an accurate electron–phonon interaction matrix.

3. Results and discussion

Crystal structures of $LaO_{0.5}F_{0.5}BiS_2$ for ambient-pressure tetragonal and high-pressure monoclinic phases are cited from Ref. [35] ($a = 4.1091$ Å, $c = 13.4196$ Å) and Ref. [18] ($a = 4.042$ Å, $b = 4.059$ Å, $c = 12.809$ Å, $\beta = 97.31°$), respectively. Here, half of the O sites are replaced by F , serving as the electron doping. Without such a replacement, the ambient-pressure structure and high-pressure structure belong to the space groups $P4/nmm$ and $P2_1/m$, respectively. The optimized results are summarized in Table 1, together with available experimental data. For the ambient-pressure tetragonal phase, the calculated structures coincide well with experimental results. However, there is a large difference between the calculation results and experimental data for high-pressure phase, which can be attributed to an obvious contrast between the pressure application of calculated (18 GPa) and experimental conditions (4 GPa).

Figure 1 shows the calculated phonon dispersions and partial phonon density of states (PDOS) for $LaO_{0.5}F_{0.5}BiS_2$ in tetragonal phase at 0 GPa, in which 30 phonon bands are extended to 430 cm^{-1}. A striking feature of this phonon spectrum is the presence of phonon softening along the A–M direction, indicating that the ambient-pressure structure of $LaO_{0.5}F_{0.5}BiS_2$ is dynamically unstable. Note that the soft phonon found here is an intrinsic property of the BiS_2 plane in tetragonal phase.[36] It is clearly seen from the PDOS that these unstable modes are directly traceable to the in-plane vibrations of S atoms, which is consistent with previous report.[37] Moreover, unstable phonon modes are intimately associated with a charge density wave instability, and conventional phonon-mediated pairing cannot explain the superconductivity of $LaO_{0.5}F_{0.5}BiS_2$ in the tetragonal phase.[38]

Table 1. Calculated lattice parameters and atomic positions of $LaO_{0.5}F_{0.5}BiS_2$ for ambient- and high-pressure phases, with related experimental results listed for comparisons.

$LaO_{0.5}F_{0.5}BiS_2$	Ambient-pressure tetragonal phase						High-pressure monoclinic phase					
	Exp.			Cal.			Exp. (4 GPa)			Cal. (18 GPa)		
a (Å)	4.1091			4.0443			4.042			3.200		
b (Å)	4.1091			4.0443			4.059			3.824		
c (Å)	13.4196			13.0889			12.809			10.140		
Atom	x	y	z	x	y	z	x	y	z	x	y	z
O/F	0	0	0	0	0	0	0.7519	0.25	–0.004	0.7253	0.2499	0.9825
S1	0.5	0	0.3844	0.5	0	0.3807	0.3970	0.25	0.3743	0.3159	0.25	0.3773
S2	0.5	0	0.8128	0.5	0	0.8133	0.1670	0.25	0.8042	–0.0208	0.2499	0.8196
La	0.5	0	0.1073	0.5	0	0.1081	0.2941	0.25	0.0997	0.4672	0.25	0.1444
Bi	0.5	0	0.6145	0.5	0	0.6136	0.1534	0.25	0.6124	0.1684	0.25	0.6123

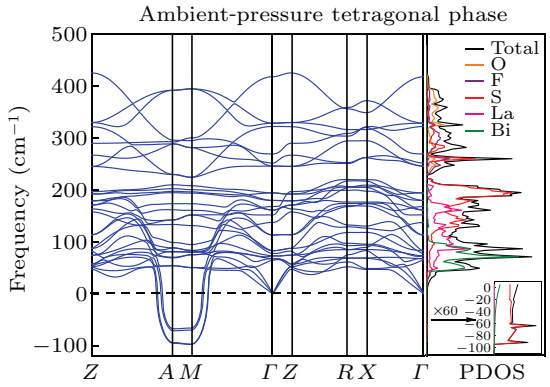


Fig. 1. Phonon dispersion curves and partial phonon density of states for $LaO_{0.5}F_{0.5}BiS_2$ in ambient-pressure tetragonal phase.

For the high-pressure monoclinic structure of $LaO_{0.5}F_{0.5}BiS_2$, we carry out the phonon calculations in a pressure range from 12 GPa to 18 GPa. The corresponding phonon dispersion curves and PDOS curves at 18 GPa are plotted in Fig. 2(a). There is no imaginary frequency in both phonon spectra, suggesting the dynamic stabilization of high-pressure phase. As seen from the phonon dispersion, the frequency extends to 700 cm^{-1}, and it can be divided into two parts. The first part is the low-frequency band, with the phonon frequency ranging from 0 cm^{-1} to 300 cm^{-1}, mainly caused by the vibrations of La and Bi atoms, while the high-frequency bands (340 cm^{-1}–700 cm^{-1}) mostly originate from the contributions of S, F, and O atoms. It is well understood that S, F, and O atoms with lighter mass usually have higher vibration frequency than Bi and La atoms. In addition, we provide a further analysis of each phonon band at the Γ point. The point group at Γ point is C1, and the Γ-point mode can be decomposed as $\Gamma = 30$ A. The detailed frequencies are listed in Table 2, with the three acoustical branches excluded.

Furthermore, in Fig. 2(b), we give the atom vibration pattern of several typical phonon bands at Γ point, whose frequencies are 181.9 cm^{-1} (A_8 mode), 477.4 cm^{-1} (A_{18} mode), and 569.8 cm^{-1} (A_{26} mode), corresponding to the three colored lines from bottom to top in Fig. 2(a). The A_8 mode corresponds to the in-plane stretching vibrations with motion along the x (y) axis. In the A_{18} mode, the O, F, and S_2 atoms vibrate along the same z direction, opposite to the vibration direction of S_1 atoms, while the A_{26} mode corresponds to the vibration of only O atom and S_2 atom.

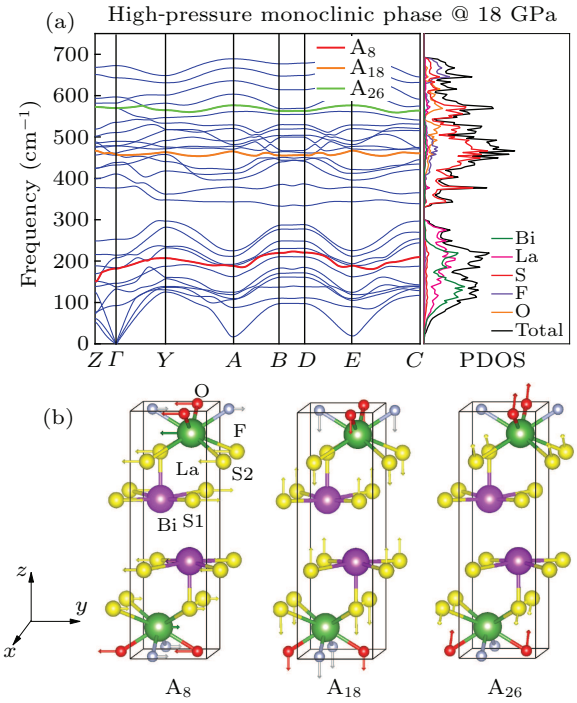


Fig. 2. (a) Phonon dispersion and projected PDOS for $LaO_{0.5}F_{0.5}BiS_2$ in high-pressure monoclinic phase at 18 GPa. (b) Atom vibration pattern of typical A_8, A_{18}, and A_{26} modes at Γ point.

Table 2. Phonon mode frequencies (in unit cm^{-1}) at Γ point for $LaO_{0.5}F_{0.5}BiS_2$ in high-pressure monoclinic phase, with I denoting infrared active, and R representing Raman active.

	Γ (0,0,0)								
A (I+R)	92.4	132.2	137.1	144.5	181.9	183.8	207.2	214.2	252.8
	375.7	410.6	432.3	438.4	455.8	457.8	459.8	477.4	477.4
	488.9	510.7	535.2	569.5	569.8	582.3	596.8	642.9	671.8

To investigate the isotope effect of $LaO_{0.5}F_{0.5}BiS_2$ in high-pressure monoclinic phase, we perform the substitution of S element. Then the $LaO_{0.5}F_{0.5}BiS_2$ samples with ^{32}S and ^{34}S isotopes are obtained, labeled as ^{32}S sample and ^{34}S sample, respectively. The effect of electron–phonon coupling on conventional superconductivity can be well represented by the Eliashberg function[39]

$$\alpha^2F(\omega) = \frac{1}{N(E_F)}\sum_{\nu\boldsymbol{q}}\sum_{nn'\boldsymbol{k}}\left|g^{\nu\boldsymbol{q}}_{n\boldsymbol{k}+\boldsymbol{q},n'\boldsymbol{k}}\right|^2\delta(\varepsilon_{n\boldsymbol{k}+\boldsymbol{q}}-E_F) \times\delta(\varepsilon_{n'\boldsymbol{k}}-E_F)\,\delta(\omega-\omega_{\nu\boldsymbol{q}}). \quad (1)$$

Here, $N(E_F)$ is the density of states at the Fermi level, ω is the frequency, n and n' run over electronic band, ν over phononic band, $\boldsymbol{k}$ and $\boldsymbol{q}$ over the Brillouin zone. The electron–phonon matrix element $\left|g^{\nu\boldsymbol{q}}_{n\boldsymbol{k}+\boldsymbol{q},n'\boldsymbol{k}}\right|^2$ is defined by the variation in the self-consistent crystal potential. Integrating the Eliashberg function over frequency, we can get the electron–phonon coupling factor λ as follows:

$$\lambda(\omega) = 2\int \mathrm{d}\omega\frac{\alpha^2F(\omega)}{\omega}. \quad (2)$$

The characteristic phonon frequency $\omega_{\ln}$ is defined as

$$\omega_{\ln} = \exp\left(\frac{\int \mathrm{d}\omega\frac{\alpha^2F(\omega)}{\omega}\ln\omega}{\int \mathrm{d}\omega\frac{\alpha^2F(\omega)}{\omega}}\right). \quad (3)$$

For $LaO_{0.5}F_{0.5}BiS_2$ in high-pressure phase with ^{32}S sample and ^{34}S sample, figure 3 shows the Eliashberg function $\alpha^2F(\omega)$ and electron–phonon coupling $\lambda(\omega)$ at 18 GPa. Combining with the PDOS in Fig. 2, it can be clearly found that the electron–phonon interaction of Bi–S bond plays a crucial role in enhancing the value of $\alpha^2F(\omega)$. Accordingly, the difference of $\alpha^2F(\omega)$ between ^{32}S sample and ^{34}S sample is mainly reflected the in high-frequency region, showing a small red-shift with the increase of isotope mass of S element. Under the pressure application of 18 GPa, both ^{32}S sample and ^{34}S sample have a factor $\lambda = 0.61$, suggesting that the $LaO_{0.5}F_{0.5}BiS_2$ in high-pressure phase is a moderately coupled electron–phonon superconductor. The values of electron–phonon coupling factor λ and the characteristic phonon frequency $\omega_{\ln}$ for ^{32}S sample and ^{34}S samples in a pressure range of 12 GPa–18 GPa are listed in Table 3. For the ^{32}S sample at 12 GPa, the value of λ is about 0.40, with the logarithmically averaged frequency $\omega_{\ln} = 271.3$ K. With the increase of pressure, the λ monotonically increases, accompanied by the decrease of $\omega_{\ln}$. In addition, the isotope substitution of S element has little influence on λ, but the values of $\omega_{\ln}$ in ^{34}S samples are generally smaller than those of ^{32}S ones. For instance, the $\omega_{\ln}$ of ^{32}S sample at 13 GPa is about 274.0 K, while it decreases to 271.4 K for ^{34}S sample.

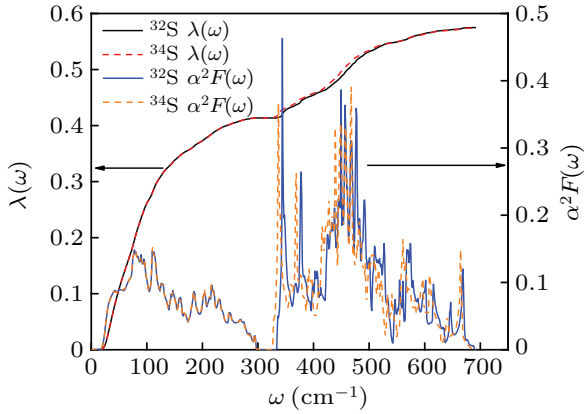


Fig. 3. Eliashberg function $\alpha^2F(\omega)$ and electron–phonon coupling $\lambda(\omega)$ for $LaO_{0.5}F_{0.5}BiS_2$ in high-pressure phase with ^{32}S sample and ^{34}S sample at 18 GPa.

Table 3. Values of electron–phonon coupling factor λ, characteristic phonon frequency $\omega_{\ln}$, and superconductive transition temperature T_c for $LaO_{0.5}F_{0.5}BiS_2$ in high-pressure phase with ^{32}S sample and ^{34}S sample in a pressure range of 12 GPa–18 GPa.

Pressure (GPa)	^{32}S sample			^{34}S sample		
	λ	$\omega_{\ln}$ (K)	T_c (K)	λ	$\omega_{\ln}$ (K)	T_c (K)
12	0.40	271.3	1.08	0.40	268.3	1.07
13	0.40	274.0	1.20	0.40	271.4	1.18
14	0.42	269.3	1.41	0.42	266.5	1.39
15	0.44	256.6	1.77	0.44	254.0	1.75
16	0.46	251.2	2.1	0.46	249.4	2.07
17	0.49	232.8	2.68	0.49	230.6	2.66
18	0.61	169.6	4.03	0.61	168.3	4.00

The effect of electron–phonon coupling on T_c is well quantified by the McMillan–Allen–Dynes formula as follows:[40]

$$T_c = \frac{\omega_{\ln}}{1.2}\exp\left[-\frac{1.04(1+\lambda)}{\lambda-\mu^*(1+0.62\lambda)}\right], \tag{4}$$

where μ^* is a pseudopotential parameter that represents the effective electron–electron mutual Coulomb repulsion suppressing pairing instability, and here $\mu^* = 0.1$. We further analyze the isotope effect of T_c by using the isotope coefficient α, which is given by

$$\alpha = -\frac{\ln[T_c]_{32_S} - \ln[T_c]_{34_S}}{\ln[M]_{32_S} - \ln[M]_{34_S}}, \tag{5}$$

in which $[M]_{32S}$ and $[M]_{34S}$ are the atomic mass of ^{32}S and ^{34}S isotopes, respectively.

The calculated T_c of $LaO_{0.5}F_{0.5}BiS_2$ in high-pressure phase for ^{32}S sample and ^{34}S sample under the pressure in a range of 12 GPa–18 GPa is displayed in Table 3. Comparing with the ^{34}S sample, the T_c of ^{32}S sample is high, which is in agreement with the isotope effect. However, the calculated T_c of $LaO_{0.5}F_{0.5}BiS_2$ in high-pressure phase is always lower than the experimental value, for example, the calculated T_c of ^{32}S sample at 18 GPa is 4.0 K, while its experimental one is 5.5 K.[18] Based on the changes of T_c between ^{32}S sample and ^{34}S sample, the isotope coefficient is exhibited in Fig. 4. It is found that the isotope coefficient of $LaO_{0.5}F_{0.5}BiS_2$ in high-pressure monoclinic phase is estimated to be $0.13 \leq \alpha \leq 0.20$, which is much greater than that of ambient-pressure phase, and slightly smaller than that of conventional MgB_2 (i.e. 0.30).[25] We thus conclude that the moderate electron–phonon coupling has a vital role in determining the superconductivity of high-pressure phase. Moreover, taking into account the calculated T_c lower than experimental value, cooperative multiple pairing mechanism should be also considered, such as electron–electron correlation.[41,42] Recalling the unconventional isotope effect of BiS_2-based superconductors in ambient-pressure structure, the switch of superconductive mechanism may ascribe to structural symmetry breaking induced by high-pressure effect. This is an impor-

tant step toward the clarification of the origin of superconductivity for BiS_2-based system in high-pressure phase. In the future, thorough research on BiS_2-based superconductors for both ambient- and high-pressure phases is very essential and necessary.

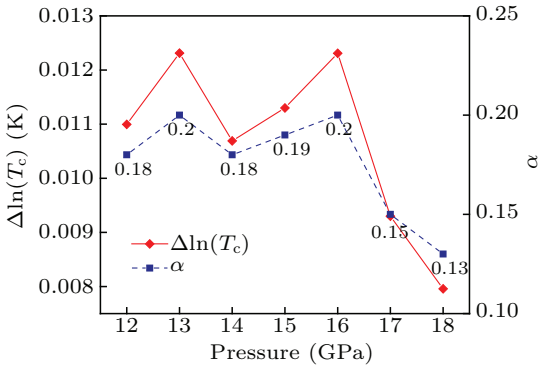


Fig. 4. Variation of T_c difference $\Delta\ln(T_c)$ between ^{32}S and ^{34}S samples, and isotope coefficient α with pressure in a range of 12 GPa–18 GPa.

4. Conclusions

Using the first-principles calculations, we reported the substitution effect of ^{32}S by the heavier isotope ^{34}S on the phonon spectra, electron–phonon coupling factor, and the superconductivity of $LaO_{0.5}F_{0.5}BiS_2$ in high-pressure monoclinic phase. The electron–phonon coupling factor can reach to 0.61, and corresponding isotope coefficient is estimated to be $0.13 \leq \alpha \leq 0.20$. It should be noted that the calculated T_c of high-pressure phase is lower than the experimental result. Therefore, we confirm the vital role of moderate phonon-mediated pairing in determining the superconductivity of high-pressure phase. However, to further clarify the nature of superconductivity in BiS_2-based superconductors, cooperative multiple paring interactions still need studying in future.

Acknowledgements

Project supported by the National Natural Science Foundation of China (Grant No. 12175107) and the Natural Science Foundation of Nanjing University of Posts and Telecommunications (Grant Nos. NY219087 and NY220038).

References

[1] Orenstein J and Millis A J 2000 *Science* **288** 468
[2] Kamihara Y, Watanabe T, Hirano M and Hosono H 2008 *J. Am. Chem. Soc.* **130** 3296
[3] Nagamatsu J, Nakagawa N, Muranaka T, Zenitani Y and Akimitsu J 2001 *Nature* **410** 63
[4] Mizuguchi Y, Fujihisa H, Gotoh Y, Suzuki K, Usui H, Kuroki K, Demura S, Takano Y, Izawa H and Miura O 2012 *Phys. Rev. B* **86** 220510
[5] Demura S, Mizuguchi Y, Deguchi C, Okazaki H, Hara H, Watanabe T, Denholme S J, Fujioka M, Ozaki T, Fujihisa H, Gotoh Y, Miura O, Yamaguchi T, Takeya H and Takano Y 2013 *J. Phys. Soc. Jpn.* **82** 033708
[6] Xing J, Li S, Ding X X, Yang H and Wen H H 2012 *Phys. Rev. B* **86** 214518
[7] Jha R, Kumar A, Kumar Singh S and Awana V P S 2013 *J. Supercond. Nov. Magn.* **26** 499
[8] Mizuguchi Y, Demura S, Deguchi K, Takano Y, Fujihisa H, Gotoh Y, Izawa H and Miura O 2012 *J. Phys. Soc. Jpn.* **81** 114725
[9] Yazici D, Huang K, White B D, Chang A H, Friedman A J and Maple M B 2013 *Phil. Mag.* **93** 673
[10] Lei H C, Wang K F, Abeykoon M, Bozin E S and Petrovic C 2013 *Inorg. Chem.* **52** 10685
[11] Goto Y, Miura A, Sakagami R, Kamihara Y, Moriyoshi C, Kuroiwa Y and Mizuguchi Y 2018 *J. Phys. Soc. Jpn.* **87** 074703
[12] Miura A, Oshima T, Maeda K, Mizuguchi Y, Moriyoshi C, Kuroiwa Y, Meng Y, Wen X D, Nagao M, Higuchi M and Tadanaga K 2017 *J. Mater. Chem. A* **5** 14270
[13] Sun Y L, Ablimit A, Zhai H F, Bao J K, Tang Z T, Wang X B, Wang N L, Feng C M and Cao G H 2014 *Inorg. Chem.* **53** 11125
[14] Jha R, Goto Y, Higashinaka R, Matsuda T D, Aoki Y and Mizuguchi Y 2018 *J. Phys. Soc. Jpn.* **87** 083704
[15] Mizuguchi Y, Hijikata Y, Abe T, Moriyoshi C, Kuroiwa Y, Goto Y, Miura A, Lee S, Torii S, Kamiyama T, Lee C H, Ochi M and Kuroki K 2017 *Europhys. Lett.* **119** 26002
[16] Paglione J and Greene R L 2010 *Nat. Phys.* **6** 645
[17] Mizuguchi Y, Demura S, Deguchi K, Takano Y, Fujihisa H, Gotoh Y, Izawa H and Miura O 2012 *J. Phys. Soc. Jpn.* **81** 114725
[18] Tomita T, Ebata M, Soeda H, Takahashi H, Fujihisa H, Gotoh Y, Mizuguchi Y, Izawa H, Miura O, Demura S, Deguchi K and Takano Y 2014 *J. Phys. Soc. Jpn.* **83** 063704
[19] Dong J, Zhang H J, Xu G, Li Z, Li G, Hu W Z, Wu D, Chen G F, Dai X, Luo J L, Fang Z and Wang N L 2008 *Europhys. Lett.* **83** 27006
[20] Mazin I I, Singh D J, Johannes M D and Du M H 2008 *Phys. Rev. Lett.* **101** 057003
[21] Bardeen J, Cooper L N and Schrieffer J R 1957 *Phys. Rev.* **108** 1175
[22] Serin B, Reynolds C A and Nesbitt L B 1950 *Phys. Rev.* **78** 813
[23] Hinks D G, Richards D R, Dabrowski B, Marx D T and MiTchell A W 1988 *Nature* **335** 419
[24] Ramirez A P, Kortan A R, Rosseinsky M J, Duclos S J, Mujsce A M, Haddon R C, Murphy D W, Makhija A V, Zahurak S M and Lyons K B 1992 *Phys. Rev. Lett.* **68** 1058
[25] Hinks D G, Claus H and Jorgensen J D 2001 *Nature* **411** 457
[26] Batlogg B, Cava R J, Jayaraman A, Dover R B V, Kourouklis G A, Sunshine S, Murphy D W, Rupp L W, Chen H S, White A, Short K T, Mujsce A M and Rietman E A 1987 *Phys. Rev. Lett.* **58** 2333
[27] Shirage P M, Kihou K, Miyazawa K, Lee C H, Kito H, Eisaki H, Yanagisawa T, Tanaka Y and Iyo A 2009 *Phys. Rev. Lett.* **103** 257003
[28] Jha R and Mizuguchi Y 2020 *Appl. Phys. Express* **13** 093001
[29] Hoshi K, Goto Y and Mizuguchi Y 2018 *Phys. Rev. B* **97** 094509
[30] Yamashita A, Usui H, Hoshi K, Goto Y, Kuroki K and Mizuguchi Y 2021 *Sci. Rep.* **11** 230
[31] Giannozzi P, Baroni S, Bonini N, *et al.* 2009 *J. Phys.: Condens. Matter* **21** 395502
[32] Baroni S, Gironcoli S, Corso A D and Giannozzi P 2001 *Rev. Mod. Phys.* **73** 515
[33] Prandini G, Marrazzo A, Castelli I E, Mounet N, Passaro E and Marzari N 2018 *NPJ Comput. Mater.* **4** 72
[34] Perdew J P, Burke K and Ernzerhof M 1996 *Phys. Rev. Lett.* **77** 3865
[35] Li B, Xing Z W and Huang G Q 2013 *Europhys. Lett.* **101** 47002
[36] Yildirim C 2013 *Phys. Rev. B* **87** 020506
[37] Wan X, Ding H C, Savrasov S Y and Duan C G 2013 *Phys. Rev. B* **87** 115124
[38] Corentin M, Ryosuke A, Takashi K, Siddharth S S and Ryotaro A 2017 *Phys. Rev. B* **95** 180505
[39] Scalapino D, in *Superconductivity*, edited by Parks R (Dekker, New York, 1969), Vol. 1, p. 449
[40] Allen P and Dynes R 1975 *Phys. Rev. B* **12** 905
[41] Ota Y, Okazaki K, Yamamoto H Q, Yamamoto T, Watanabe S, Chen C T, Nagao M, Watauchi S, Tanaka I, Takano Y and Shin S 2017 *Phys. Rev. Lett.* **118** 167002
[42] Liang Y, Wu X X, Tsai W F and Hu J P 2014 *Front. Phys.* **9** 194